Journal of the Korean Crystal Growth and Crystal Technology
Vol. 17, No. 6 (2007) 256-263

Ground-based model study for spaceflight experiments under microgravity environments on thermo-solutal convection during physical vapor transport of mercurous chloride

Jeong-Gil Choi†, Kyong-Hwan Lee* and Geug-Tae Kim

Department of Nano-Bio Chemical Engineering, Hannam University, Daejeon 305-811, Korea
**Fossil Energy Environment Research Department, Korea Institute of Energy Research, Taejon 305-343, Korea*

(Received October 12, 2007)
(Accepted October 29, 2007)

Abstract For $P_B = 50$ Torr, $P_T = 5401$ Torr, $T_S = 450^oC$, $\Delta T = 20$ K, Ar = 5, Pr = 3.34, Le = 0.01, Pe = 4.16, Cv = 1.05, adiabatic and linear thermal profiles at walls, the intensity of solutal convection (solutal Grashof number $Grs = 7.86 \times 10^6$) is greater than that of thermal convection (thermal Grashof number $Grt = 4.83 \times 10^5$) by one order of magnitude, which is based on the solutally buoyancy-driven convection due to the disparity in the molecular weights of the component A (Hg_2Cl_2) and B (He). With increasing the partial pressure of component B from 20 up to 800 Torr, the rate is decreased exponentially. It is also interesting that as the partial pressure of component B is increased by a factor of 2, the rate is approximately reduced by a half. For systems under consideration, the rate increases linearly and directly with the dimensionless Peclet number which reflects the intensity of condensation and sublimation at the crystal and source region. The convective transport decreases with lower g level and is changed to the diffusive mode at 0.1 g_0. In other words, for regions in which the g level is 0.1 g_0 or less, the diffusion-driven convection results in a parabolic velocity profile and a recirculating cell is not likely to occur. Therefore a gravitational acceleration level of less than 0.1 g_0 can be adequate to ensure purely diffusive transport.

Key words Mercurous chloride, Thermo-solutal convection, Physical vapor transport, Microgravity environments, Ground-based model study, Spaceflight experiments

1. Introduction

Mercurous chloride (Hg_2Cl_2) is a heavy metal halide material of potential commercial importance. As compared with traditional commercial materials such Te_2O_2, $PbMoO_4$, $LiNbO_3$, $AgAsS_3$ and quartz, Hg_2Cl_2 has many advantages in its applications to acousto-optic (A-O), and opto-electronic devices. These advantages arise primarily from the fact that Hg_2Cl_2 has the unique properties of a broad transmission range from 0.36 to 20 μm, well into the far infra-red, a low acoustic velocity, a high signal-to-noise ratio (SNR), and relatively large birefringence [1]. The equimolar Hg_2Cl_2 compound decomposes to two liquids at a temperature near 525°C where the vapor pressure is well above 20 atm [2, 3]. Because of this decomposition and high vapor pressure, Hg_2Cl_2 cannot be solidified as a single crystal directly from the stoichiometric melt. Given sufficiently high vapor pressure at temperatures below its melting point, mercurous chloride can be sublimed and, after transport through a vapor space, recondensed in a single crystalline form. This technique, when performed in closed silica glass ampoules, is referred to as crystal growth by physical vapor transport (PVT). It is technically simple, requires minimal process control and monitoring, and transport results are easily interpreted. Therefore, recently PVT has been extensively used for materials processing experiments for a variety of acousto-optic materials in low gravity environments. However, the industrial applications of the PVT process remain limited. One of important main reasons is that transport phenomena occurring in the vapor are complex and coupled so that it is difficult to design or control the process accurately. Such complexity and coupling are associated with the inevitable occurrence of thermal and/or solutal convection generated by the interaction of gravity with density gradients arising from temperature and/or concentration gradients. In general, convection has been regarded as detrimental and, thus, to be avoided or minimized in PVT growth system. These thermal and/or solutal convection-induced complications result in problems ranging from crystal inhomogeneity to structural imperfection. Therefore, in order to analyze and control the PVT process accurately, and also make significant improvements in the process, it is essential to

†Corresponding author
Tel: +82-42-629-8841
Fax: +82-42-629-8835
E-mail: jgchoi@hannam.ac.kr

investigate the roles of convection in the PVT process.

Markham, Greenwell and Rosenberger [4] examined the effects of thermal and thermosolutal convections during the PVT process inside vertical cylindrical enclosures for a time-independent system, and showed that even in the absence of gravity, convection can be present, causing nonuniform concentration gradients. They emphasized the role of geometry in the analysis of the effects of convection. As such these fundamentally constitute steady state two-dimensional models. The steady state models are limited to low Rayleigh number applications, because as the Rayleigh number increases oscillation of the flow field occurs. To address the issue of unsteady flows in PVT, Duval [5] performed a numerical study on transient thermal convection in the PVT processing of Hg_2Cl_2 very similar to the mercurous bromide for a vertical rectangular enclosure with insulated temperature boundary conditions for Rayleigh numbers up to 10^6. Nadarajah *et al.* [6] addressed the effects of solutal convection for any significant disparity in the molecular weights of the crystal components and the inert gas. Zhou *et al.* [7] reported that the traditional approach of calculating the mass flux assuming one-dimensional flow for low vapor pressure systems is indeed correct. Rosenberger *et al.* [8] studied three-dimensional numerical modeling of the PVT yielded quantitative agreement with measured transport rates of iodine through octofluorocyclobutane (C_4F_8) as inert background gas in horizontal cylindrical ampoules. We reported the effect of accelerational perturbations on physical vapor transport crystal growth under microgravity environments, which was focused on the linear temperature profiles at walls and relatively low temperature ranges from 330 and 340°C [9].

In this theoretical study, a two-dimensional model is used for the analysis of the PVT processes during vapor-growth of mercurous chloride crystals (Hg_2Cl_2) in horizontally oriented, cylindrical, closed ampoules in a two-zone furnace system. Diffusion-limited processes are considered in this paper, although the recent paper of Singh, Mazelsky and Glicksman [10] demonstrated that the interface kinetics plays an important role in the PVT system of Hg_2Cl_2. Solutally buoyancy-driven convection will be considered at this point, primarily for a mixture of Hg_2Cl_2 vapor and impurity of Helium (He). Thermal convection is negligible in comparison to solutally-induced convection for adiabatic conditions and imposed linear thermal profiles at walls to prevent supersaturation along the transport path.

It is the purpose of this paper to relate applied thermo-solutally buoyancy-driven convection process parameters such as a partial pressure of component B (He), an aspect ratio (transport length-to-width), a gravitational level at two different wall boundary conditions, i.e., adiabatic and linear temperature profiles at walls, to the crystal growth rate and the maximum velocity magnitude in order to gain insights into the underlying physicochemical processes.

2. The Model

We restrict our model to examine how a typical solutally buoyancy-driven convection will affect the crystal growth rate and its distributions across an interface, and the maximum magnitude of velocity vector. We consider a rectangular enclosure of height H and transport length L, shown in Fig. 1. The source is maintained at a temperature T_s, while the growing crystal is at a temperature T_c, with $T_s > T_c$. PVT of the transported component A (Hg_2Cl_2) occurs inevitably, due to presence of impurities, with the presence of a component B (He). The transport of fluid within a rectangular PVT crystal growth reactor is governed by a system of elliptic, coupled conservation equations for mass (continuity), momentum, energy and species (diffusion) with their appropriate boundary conditions. Let v_x, v_y denote the velocity components along the x- and y-coordinates in the x, y rectangular coordinate, and let T, ω_A, p denote the temperature, mass fraction of species A (Hg_2Cl_2) and pressure, respectively. The detailed physical and mathematical formulations could be found in refs. [11, 12].

The dimensionless variables are scaled as follows:

$$x^* = \frac{x}{H}, \quad y^* = \frac{y}{H}, \tag{1}$$

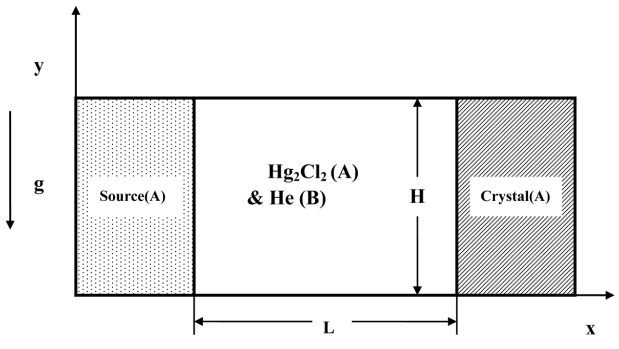

Fig. 1. Schematic of PVT growth reactor in a two-dimensional rectangular system.

$$u = \frac{u_x}{U_c},\ v = \frac{v_y}{U_c},\ p = \frac{p}{\rho_c U_c^2}, \tag{2}$$

$$T^* = \frac{T-T_c}{T_s-T_c},\ \omega_A^* = \frac{\omega_A-\omega_{A,c}}{\omega_{A,s}-\omega_{A,c}}. \tag{3}$$

The dimensionless governing equations are given by:

$$\nabla^* \bullet V^* = 0, \tag{4}$$

$$\vec{V}^* \bullet \nabla^* \vec{V}^* = -\nabla^* p^* + Pr\nabla^{*2}\vec{V}^* - Ra \cdot Pr \cdot T^* \cdot e_g, \tag{5}$$

$$\vec{V}^* \bullet \nabla^* T^* = \nabla^{*2} T^* \tag{6}$$

$$\vec{V}^* \bullet \nabla^* \omega_A^* = \frac{1}{Le}\nabla^{*2}\omega_A^* \tag{7}$$

These nonlinear, coupled sets of equations are numerically integrated with the following boundary conditions:

On the walls ($0 < x^* < L/H$, $y^* = 0$ and 1):

$$u(x^*,0) = u(x^*,1) = v(x^*,0) = v(x^*,1) = 0 \tag{8}$$

$$\frac{\partial \omega_A^*(x^*,0)}{\partial y^*} = \frac{\partial \omega_A^*(x^*,1)}{\partial y^*} = 0,$$

$$T^*(x^*,0) = T^*(x^*,1) = \frac{T-T_c}{T_s-T_c}: \text{conducting}$$

$$\frac{\partial T^*(x^*,0)}{\partial y^*} = \frac{\partial T^*(x^*,1)}{\partial y^*} = 0: \text{adiabatic}$$

On the source ($x^* = 0$, $0 < y^* < 1$):

$$u(0,y^*) = -\frac{1}{Le}\frac{\Delta\omega}{(1-\omega_{A,s})}\frac{\partial \omega_A^*(0,y^*)}{\partial x^*}, \tag{9}$$

$$v(0,y^*) = 0,$$

$$T^*(0,y^*) = 1,$$

$$\omega_A^*(0,y^*) = 1.$$

On the crystal ($x^* = L/H$, $0 < y^* < 1$):

$$u(L/H,y^*) = -\frac{1}{Le}\frac{\Delta\omega}{(1-\omega_{A,c})}\frac{\partial \omega_A^*(L/H,y^*)}{\partial x^*} \tag{10}$$

$$v(L/H,y^*) = 0,$$

$$T^*(L/H,y^*) = 0,$$

$$\omega_A^*(L/H,y^*) = 0.$$

3. Results and Discussion

One of the purposes for this study is to correlate the growth rate to process parameters such as a partial pressure of component B (He), an aspect ratio, a gravitational level with a linear temperature profile. Thus, it is desirable to express some results in terms of dimensional growth rate, however they are also applicable to parameter ranges over which the process varies in the manner given. The six dimensionless parameters, namely Gr, Ar, Pr, Le, C_v and Pe, are independent and arise naturally from the dimensionless governing equations and boundary conditions. The dimensionless parameters and physical properties for the operating conditions of this study are shown in Table 1.

Table 1
Typical thermo-physical properties and operating conditions used in this study (M_A = 472.086 g/mol, M_B = 4.003 g/mol)

Ampoule transport length, L	5 cm
Ampoule height, H	1 cm
Source temperature, T_s	450°C
Crystal temperature, T_c	430°C
Gravitational acceleration (g_0)	9.81 m/s^2
Density, ρ	0.043 g/cm^3
Dynamic viscosity, μ	0.000325 g/(cm²sec)
Diffusivity, D_{AB} (at P_T = 5401 Torr)	0.22 cm^2/s
Thermal expansion coefficient, β	0.00138 K^{-1}
Prandtl number, Pr	3.34
Lewis number, Le	0.01
Peclet, Pe	4.16
Concentration number, Cv	1.01
Total system pressure, P_T	5401 Torr
Partial pressure of component B, P_B	50 Torr
Thermal Grashof number, Gr_t	4.83×10^5
Solutal Grashof number, Gr_s	7.86×10^6

When the molecular weight of a light element (He) is not equal to that of the crystal component (Hg_2Cl_2) during the physical vapor transport, both solutal and thermal effects should be considered. If solutal convection is dominant, the imposed temperature profile has little effect on the growth rate [6]. Even though most of vapor growth experiments are performed under the imposed nonlinear thermal profile to avoid nucleation at the ampoule walls, in this study adiabatic and conductive wall boundary conditions with a linear thermal profile are considered for simplicity. Note that the adiabatic wall boundary conditions are difficult to obtain in practice. Moreover, a linear temperature profile is rarely used in practice because the vapor of component A (Hg_2Cl_2) is in a supersaturation throughout the ampoule.

Figure 2 shows the effect of partial pressure of component B (Helium), P_B (Torr) on the crystal growth rates of Hg_2Cl_2, for Ar = 5, ΔT = 20 K, P_T = 5401 Torr, Grt = 4.83×10^5, Grs = 7.86×10^6, P_B = 50 Torr, Pr = 3.34, Le = 0.01, Pe = 4.16, Cv = 1.01. Figure 2 is based on the adiabatic walls. With increasing the partial pressure of component B from 20 up to 800 Torr, the rate is decreased exponentially by a first order. The addition of

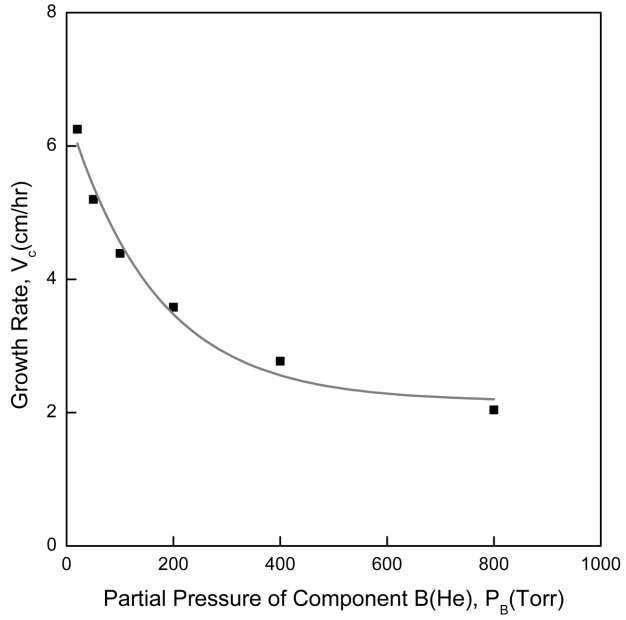

Fig. 2. The effect of partial pressure of component B (Helium), P_B (Torr) on the crystal growth rates of Hg_2Cl_2, for Ar = 5, ΔT = 20 K, P_T = 5401 Torr, Grt = 4.83 × 10^5, Grs = 7.86 × 10^6, P_B = 50 Torr, Pr = 3.34, Le = 0.01, Pe = 4.16, Cv = 1.01. Based on the adiabatic walls.

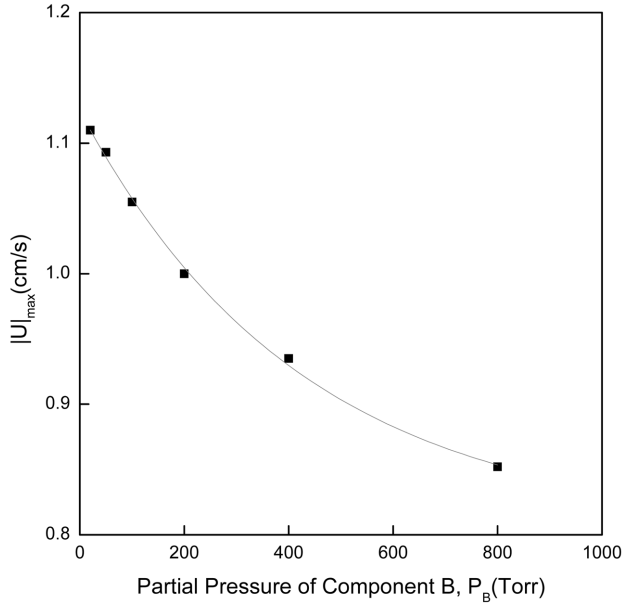

Fig. 3. The effect of partial pressure of component B (Helium), P_B (Torr) on the maximum velocity magnitude, $|U|_{max}$, corresponding to Fig. 2.

the helium component results in an increase in total pressure, which causes the thermophysical variations of density and binary diffusion coefficient. Assuming that the Hg_2Cl_2 vapor is incompressible in the pressure ranges considered in the PVT process, the binary diffusion coefficient D_{AB} is dependent on pressure, i.e., D_{AB}~1/P.

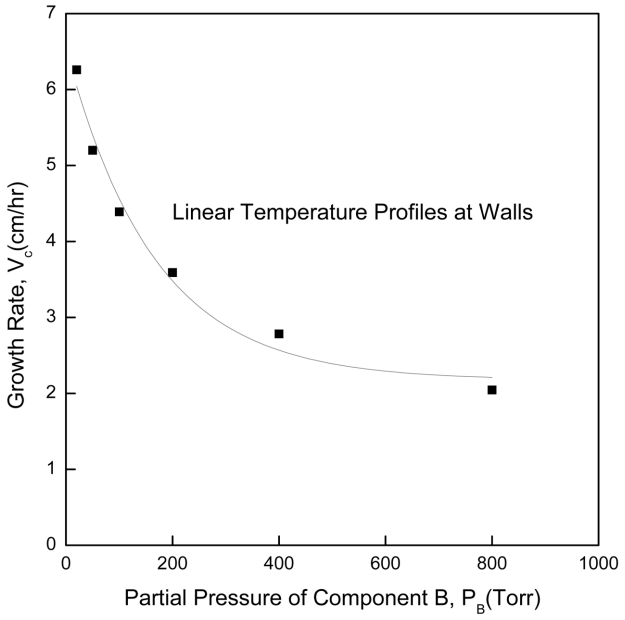

Fig. 4. The effect of partial pressure of component B (Helium), P_B (Torr) on the crystal growth rates of Hg_2Cl_2, for Ar = 5, ΔT = 20 K, T_s = 450, P_T = 5401 Torr, Grt = 4.83 × 10^5, Grs = 7.86 × 10^6, P_B = 50 Torr, Pr = 3.34, Le = 0.01, Pe = 4.16, C_v = 1.01. Based on the linear temperature profiles at walls.

Moreover, the increase in the partial pressure of inert gas (component He) results in the decrease of mass fraction of Hg_2Cl_2 at both interfaces. As a result, the mass flux is reduced. From this consideration, the addition of inert gas in the PVT systems can alter the convective state. Therefore, the effect of partial pressure of component B (helium) is in the main reflected through the binary diffusion coefficient. In other words, as the partial pressure of B is increased, the binary diffusion coefficient is decreased so that the mass transfer by diffusion would be reduced. Figure 3 shows the effect of the partial pressure of B on the maximum velocity magnitude, $|U|_{max}$ corresponding to Fig. 2. As shown in Fig. 3, the same trend for the maximum velocity magnitude appears as for the rate in Fig. 2. From Figs. 2 and 3, the rates for the partial pressures above the 600 Torr are likely to be invariant. Also, as the partial pressure of component B increases from 20 Torr to 100 Torr, the rate is reduced by a factor of a half. Moreover, with a decrease of the P_B, the $|U|_{max}$ increases due to the large sublimation and condensation velocities characterized by the Peclet number. As the total pressure decreases, the Peclet number is increased and the Grashof number is decreased slightly due to the slight variations of density. Note that for very low partial pressures of component B, the total pressure does not change, thus the Grashof number remains constant.

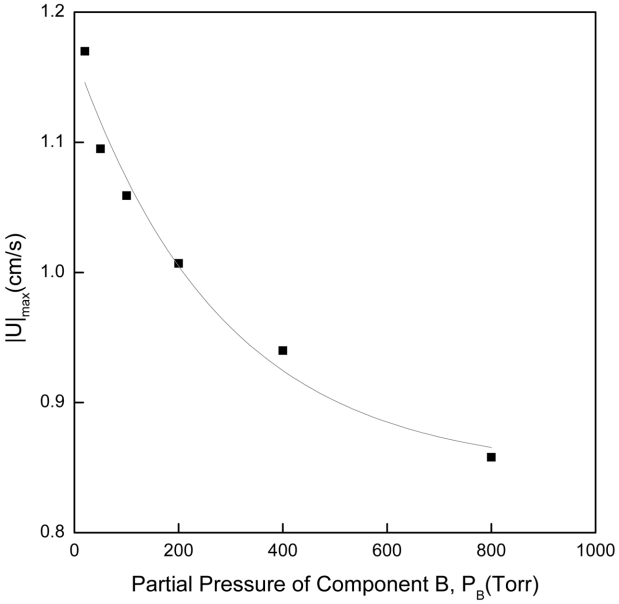

Fig. 5. The effect of partial pressure of component B (Helium), P_B (Torr) on the maximum velocity magnitude, $|U|_{max}$, corresponding to Fig. 4.

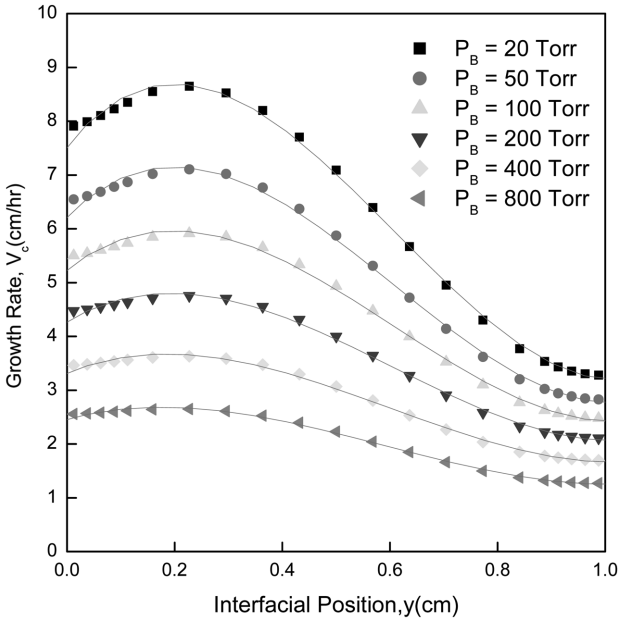

Fig. 6. Interfacial distribution of the crystal growth rates of Hg_2Cl_2 for the various partial pressures of component B (Helium), P_B = 20, 50, 100, 200, 400, 800 Torr. Based on the adiabatic walls, Ar = 5, ΔT = 20 K, T_s = 450, P_T = 5401 Torr.

Figure 4 shows the effect of partial pressure of component B (Helium), P_B (Torr) on the crystal growth rates of Hg_2Cl_2, for Ar = 5, ΔT = 20 K, P_T = 5401 Torr, Grt = 4.83×10^5, Grs = 7.86×10^6, P_B = 50 Torr, Pr = 3.34, Le = 0.01, Pe = 4.16, Cv = 1.01. Figure 4 is based on linear temperature profiles at walls. Figure 5 illustrates the effect of partial pressure of component B (Helium), P_B

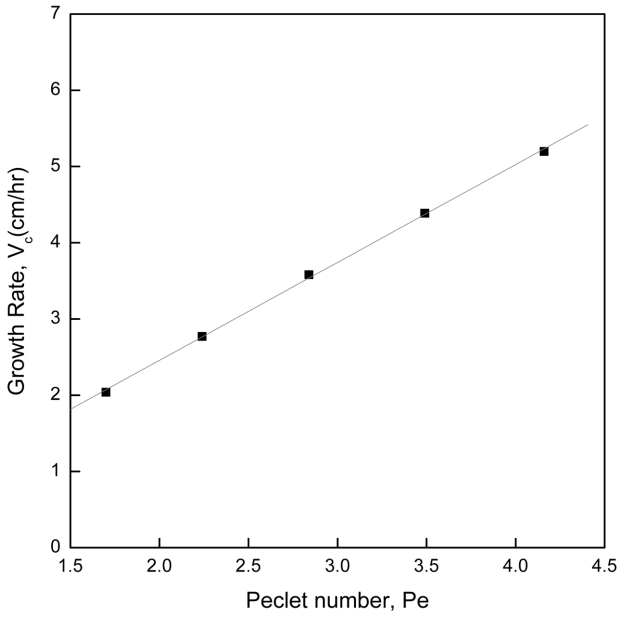

Fig. 7. Growth rates of Hg_2Cl_2 as a function of the dimensionless Peclet number, Pe, for Ar = 5, ΔT = 20 K, T_s = 450, P_T = 5401 Torr, with adiabatic walls and horizontal orientation against the gravitational vector.

(Torr) on the maximum velocity vector magnitude, corresponding to Fig. 4. Compared with Figs. 2 and 3, Figs. 4 and 5 shows the growth rate and the $|U|_{max}$ for the linear thermal boundary condition are slightly greater than those for the adiabatic conditions. This indicates the intensity of thermo-solutal convection for the former is stronger than for the latter.

Figure 6 shows the interfacial distribution of the crystal growth rates of Hg_2Cl_2 for the various partial pressures of component B (Helium), P_B = 20, 50, 100, 200, 400, 800 Torr, Ar = 5, ΔT = 20 K, T_s = 450, P_T = 5401 Torr, with the adiabatic walls. As the addition of inert gas B increases, the variations in the growth rate are reduced throughout the interfacial ranges, $0 \le y \le 1$ cm. The maximum of growth rate appears in the neighborhood of y = 0.2 for $20 \le P_B \le 800$ Torr, which indicates the same structure of convective flow, even if the corresponding convective flow patterns are not shown in this paper. It is also interesting that as the partial pressure of component B is increased by a factor of 2, the rate is approximately reduced by a half. Figure 7 shows that growth rates of Hg_2Cl_2 as a function of the dimensionless Peclet number, Pe, for Ar = 5, ΔT = 20 K, T_s = 450, P_T = 5401 Torr, with adiabatic walls and horizontal orientation against the gravitational vector. The rate increases linearly and directly with the dimensionless Peclet number which reflects the intensity of condensation and sublimation at the crystal and source region. Figure 8 shows

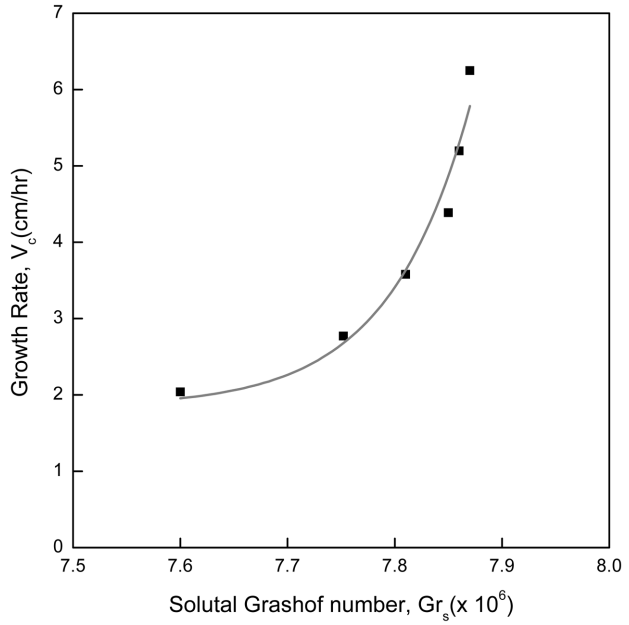

Fig. 8. Growth rates of Hg_2Cl_2 as a function of the dimensionless solutal Grashof number, Grs, for Ar = 5, ΔT = 20 K, T_s = 450, P_T = 5401 Torr, with adiabatic walls and horizontal orientation against the gravitational vector.

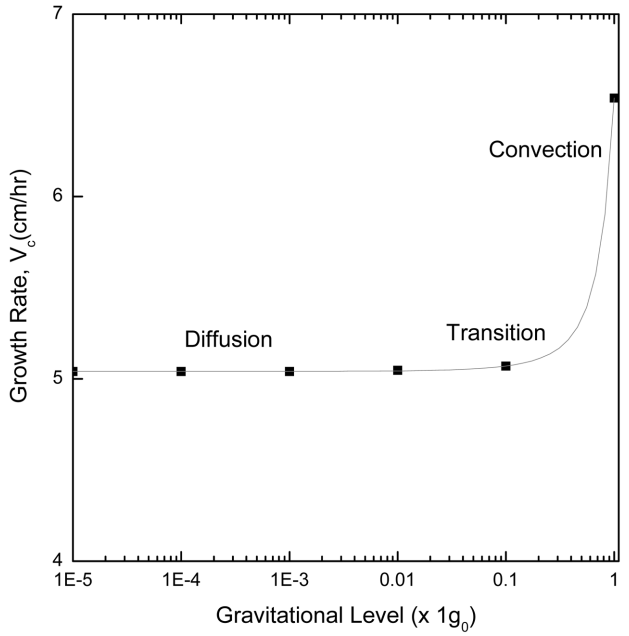

Fig. 9. The effect of the gravitational level on the growth rate of Hg_2Cl_2, for $10^{-5} g_0 \le g \le 1\ g_0$.

that growth rates of Hg_2Cl_2 as a function of the dimensionless solutal Grashof number, Grs, for Ar = 5, ΔT = 20 K, T_s = 450, P_T = 5401 Torr, with adiabatic walls and horizontal orientation against the gravitational vector. As shown in Fig. 8, the rate increases exponentially with increasing the solutal Grashof number, which means the intensity of solutally buoyancy-driven convection. For Figs. 2 through 7, the process parameters are based on P_T = 5401 Torr, T_S = 450, T = 20 K, Ar = 5, Pr = 3.34, Le = 0.01, Pe = 4.16, Cv = 1.05. The intensity of solutal convection is greater than that of thermal convection by one order of magnitude.

From the viewpoint of effect of gravitational level on the growth rate and the maximum velocity magnitude, one of the possible alternatives is to grow the crystal in a microgravity environment. The microgravity environment is of interest for research on vapor-crystal growth because solutally buoyancy-driven convection and hydrostatic pressure can be virtually reduced or eliminated. We have simulated different levels of gravity. Figure 9 shows our results for a horizontal system of aspect ratio 5 (L = 5 cm, H = 1 cm), with a source temperature T_s = 450°C, a crystal temperature T_c = 430°C, a total pressure of 5401 Torr and an acceleration of $1g_0$ in the positive y-direction, where g_0 denotes the Earth's gravitational acceleration. Similar to the earlier finding of Markham, Greenwell and Rosenberger [4], one sees that the convective flow can cause significant nonuniformities in the growth rate, with the specific distribution revealing dominance of solutal convection. The specific observation for space processing is that with the reduction in gravitational acceleration to 0.1 g_0, diffusion transport dominates over convection as well as under the ground environment. For the process conditions under considerations, the variations in the growth rates throughout the interfacial regions for horizontally positioned 1 g_0 are found to be nearly invariant, which indicates diffusion-transport relatively dominated over convective transport. Strictly speaking, as shown in Figs. 8 and 9, the diffusive transport can be obtained below 0.1 g_0, which is unlike other crystal growth methods being tested in low gravity environments, requiring gravitational levels of 10^{-5} g_0 or lower to avoid convective effects [13]. Figure 9 shows the sensitivity of the growth rate to the variations of the gravity level between 10^{-6} g_0 and 1 g_0 for a horizontal configuration with Ar = 5 and ΔT = 20 K. The effect of convection decreases with decreasing values of the gravity level, shown in Figs. 9 and 10. In particular, as the level of gravity decreases, there is a sharp decrease of a crystal growth rate near the 1 g_0 and a much more gradual decrease thereafter. The dimensional maximum magnitude of velocity ($|U|_{max}$) for the gravity level in Fig. 10 is 1.45 cm/s; for 0.1 g_0, 0.663 cm/s. As one sees in Fig. 10, the convective transport decreases with lower g level and is changed to the diffusive mode at 0.1 g_0. For regions in which the g

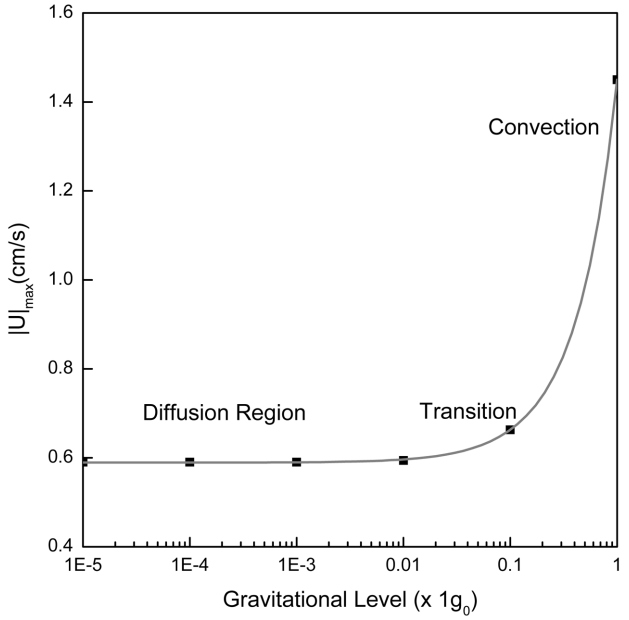

Fig. 10. The effect of the gravitational level on the maximum velocity magnitude, $|U|_{max}$, for 10^{-5} $g_0 \leq g \leq 1$ g_0, corresponding to Fig. 9.

level is 0.1 g_0 or less, the diffusion-driven convection results in a parabolic velocity profile and a recirculating cell does not occur (not shown). In general, even for situations of purely diffusive transport the rate was not strictly uniform, with growth being greater near the center than the edges. Therefore convective effects can easily be suppressed in physical vapor transport systems for most low gravity environments. A gravitational acceleration level of less than 0.1 g_0 can be adequate to ensure purely diffusive transport.

4. Conclusions

For $P_B = 50$ Torr, $P_T = 5401$ Torr, $T_S = 450^oC$, $\Delta T = 20$ K, Ar = 5, Pr = 3.34, Le = 0.01, Pe = 4.16, Cv = 1.05, adiabatic and linear thermal profiles at walls, the intensity of solutal convection (solutal Grashof number Grs = 7.86×10^6) is greater than that of thermal convection (thermal Grashof number Grt = 4.83×10^5) by one order of magnitude, which is based on the solutally buoyancy-driven convection due to the disparity in the molecular weights of the component A (Hg_2Cl_2) and B (He). With increasing the partial pressure of component B from 200 up to 800 Torr, the rate is decreased exponentially. The addition of the helium component results in an increase in total pressure, which causes the thermophysical variations of density and binary diffusion coefficient. It is also interesting that as the partial pressure of component B is increased by a factor of 2, the rate is approximately reduced by a half. For systems under consideration, the rate increases linearly and directly with the dimensionless Peclet number which reflects the intensity of condensation and sublimation at the crystal and source region.The convective transport decreases with lower g level and is changed to the diffusive mode at 0.1 g_0. In other words, for regions in which the g level is 0.1 g_0 or less, the diffusion-driven convection results in a parabolic velocity profile and a recirculating cell is not likely to occur. Therefore convective effects can easily be suppressed in physical vapor transport systems for most low gravity environments. A gravitational acceleration level of less than 0.1 g_0 can be adequate to ensure purely diffusive transport.

Acknowledgement

This study was financially supported by the Hannam University through the Kyobi program of research project number of 2007A040 (April 1, 2007 through March 31, 2008).

References

[1] N.B. Singh, M. Gottlieb, G.B. Brandt, A.M. Stewart, R. Mazelsky and M.E. Glicksman, "Growth and characterization of mercurous halide crystals:mercurous bromide system," J. Crystal Growth 137 (1994) 155.
[2] N.B. Singh, R.H. Hopkins, R. Mazelsky and J.J. Conroy, "Purification and growth of mercurous chloride single crystals," J. Crystal Growth 75 (1970) 173.
[3] S.J. Yosim and S.W. Mayer, "The mercury-mercuric chloride system," J. Phys. Chem. 60 (1960) 909.
[4] B.L. Markham, D.W. Greenwell and F. Rosenberger, "Numerical modeling of diffusive-convective physical vapor transport in cylindrical vertical ampoules," J. Crystal Growth 51 (1981) 426.
[5] W.M.B. Duval, "Convection in the physical vapor transport process-- I: Thermal," J. Chemical Vapor Deposition 2 (1994) 188.
[6] A. Nadarajah, F. Rosenberger and J. Alexander, "Effects of buoyancy-driven flow and thermal boundary conditions on physical vapor transport," J. Crystal Growth 118 (1992) 49.
[7] H. Zhou, A. Zebib, S. Trivedi and W.M.B. Duval, "Physical vapor transport of zinc-telluride by dissociative sublimation," J. Crystal Growth 167 (1996) 534.
[8] F. Rosenberger, J. Ouazzani, I. Viohl and N. Buchan, "Physical vapor transport revised," J. Crystal Growth 171 (1997) 270.
[9] J.-G. Choi, K.-H. Lee, M.-H. Kwon and G.-T. Kim,

"Effect of accelerational perturbations on physical vapor transport crystal growth under microgravity environments", J. Korean Crystal Growth and Crystal Technology 16 (2006) 203.

[10] N.B. Singh, R. Mazelsky and M.E. Glicksman, "Evaluation of transport conditions during PVT: mercurous chloride system," PhysicoChemical Hydrodynamics 11 (1989) 41.

[11] G.-T. Kim and K.-H. Lee, "Parametric studies on convection during the physical vapor transport of mercurous chloride (Hg_2Cl_2)", J. Korean Crystal Growth and Crystal Technology 14 (2004) 281.

[12] G.T. Kim, "Convective-diffusive transport in mercurous chloride (Hg_2Cl_2) crystal growth ," J. Ceramic Processing Research 6(2005) 110.

[13] A. Nadarajah, F. Rosenberger and J. Alexander, "Modelling the solution growth of TGS crystals in low gravity," J. Crystal Growth 104 (1990) 218.